RSC Advances

ROYAL SOCIETY OF CHEMISTRY

www.rsc.org/advances

Cite this: DOI: 10.1039/c0xx00000x

www.rsc.org/xxxxxx

ARTICLE TYPE

Excellent friction-reducing performance of superhydrophobic steel surface in dry sliding

Yang Li,[a] Yong Wan,*[a] Zhiwei Dong,[a] and Junyan Zhang[b]

Received (in XXX, XXX) Xth XXXXXXXXX 200X, Accepted Xth XXXXXXXXX 200X

DOI: 10.1039/b000000x

Superhydrophobic micro/nano-engineered steel surfaces with friction-reducing performances were fabricated by the combination of chemical etch and stearic acid coating. The chemical etching technique was used to produce micro/ nano-textured steel surfaces, while stearic acid coating was used to lower the surface energies of the textured surfaces. The wetting properties of the micro/nano-engineered steel surfaces were studied using a contact angle measurement system. The frictional properties of the micro/nano-engineered steel surfaces were investigated using a tribotester in ball-on-plate configuration. This study shows that the frictional performances of micro/ nano-textured steel are significantly improved compared to untreated steel surfaces.

Introduction

Superhydrophobicity, firstly observed on lotus leaves, has inspired researchers around the world [1-12]. The superhydrophobic surfaces possess special properties and may find promising applications in self-cleaning [13,14], anticorrosion [15-17], anti-icing [18-24], and so forth. It is known that the wettability of a solid surface is governed by both surface chemical composition and surface geometrical microstructures. To fabricate a superhydrophobic surface with a water contact angle (CA) larger than 150°, these two key factors must be considered. The hydrophobicity is enhanced when the surface energy is lowered. However, even the material with the lowest surface energy gives a water CA of only around 120°. Generally, very large CAs and a superhydrophobic behaviour can be determined only if surface simultaneously possesses low surface energy and elevated roughness.

In fact, these two key factors in determining surface wettability also play great role in affecting surface frictional behavior. Materials at elevated roughness and/or with low surface energy are beneficial in reducing friction in sliding contact. In the past, artificial creation of certain micro- and/or nanometer-scale surface structures, known as surface texturing technology in tribology community, are explored to reduce friction in the sliding contact. It can be found that textures on relatively flat surfaces was very effective in reducing micro-/nanoscale adhesion and friction of the materials in both dry and lubricated conditions [25–28]. Furthermore, reducing surfaces energy is also reported as an effective way to decrease the friction. For example, fluorine-containing terminal alkyne-derived monolayers on silicon substrate combines excellent hydrophobicity, low adhesion and low friction, making these highly promising candidates for use in high-performance microelectronic devices [29]. When a topographically modified surface is coated with a film with low surface energy, the superhydrophobic surface obtained would be capable of integrating the advantages of these two treatments and possess excellent tribological properties. Therefore, from the viewpoint of tribology, the design of superhydrophobic surfaces is expected to reach low friction for materials. In fact, few studies have been performed to concern tribological performances of superhydrophobic surface [30-33].

In this manuscript, we present a simple two-step route to construct superhydrophobic surfaces on carbon steel, an important materials in industrial. A rough surface with a certain micro- and nanometer-scale structures is firstly prepared on steel by chemical etch. The as-obtained rough surface is then coated with a stearic acid film in the second step to achieve superhydrophobic properties to steel surface. The mechanical and friction-reducing properties of superhydrophobic surface on steel were examined.

Results and discussion

Fabrication of superhydrophobic film on steel

To fully characterize and understand the friction-reducing performance of steel superhydrophobic surfaces generated by combining chemical etch and stearic acid coating in our process, it is necessary to first examine the means by which surface roughness is created. The mechanisms of the chemical etch step defines the size, distribution, roughness and stability of the structures. Therefore, prior to presenting tribological measurement data, we discuss in detail the chemical and physical effects of the etching on the steel. A mixture of hydrofluoric acid (HF) and hydrogen peroxide (H_2O_2) was used to create the rough steel surface. The etch process occurs through competing HF etching and H_2O_2 passivation reactions, which continue until the surface has been fabricated.

Fig. 1 presents XPS spectra for fluorine, oxygen and iron on

steel after etching. Close inspection of the XPS spectra reveals the formation of FeF_3 (685.7 and 714.2 eV) along with Fe_2O_3 (710.9eV) on the surface. The similar XPS results have been reported previous for stainless steel etched by HF [34]. During the etch process, the steel samples change from their well-known, shiny silver appearance to black due to the added surface roughness and changes in chemical surface composition. Simultaneously, the HF acid solution turns green, a color that is characteristic of FeF_3.

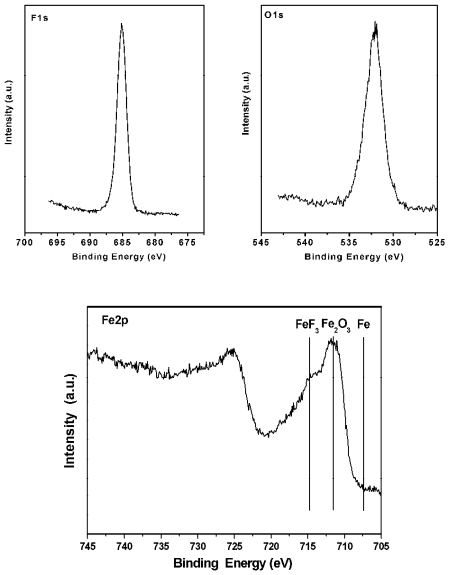

Fig. 1. XPS scans of F1s, O1s and Fe2p of superhydrophobic film on steel.

Through the deposition of FeF_3 and Fe_2O_3 on the steel surface, roughness is created at micrometer and submicrometer lengths. Fig. 2 shows surface texture of steel before and after chemical etch as observed by SEM. Whereas the nonetched sample is smooth with no significant topographical features with roughness of *Ra* and *Rz* values of 0.52 and 2.5 μm, respectively (Fig. 2a), a distinctive texture is clearly seen on the etched surface. In fact, iron fluoride has been reported to have granular crystalline structures, similar to those shown in Figure 2. The surface roughening is also visible in roughness of *Ra* and *Rz* values of 1.23 and 5.3 μm, respectively, for etched steel surface.

To fabricate a superhydrophobic surface on steel, a stearic acid coating was applied to etched steels by immersing them in the ethanol solution containing stearic acid molecules for 24h. The wetting properties were evaluated by water contact angle measurements of the samples surfaces. Fig. 3 shows the shape of a water droplet on steel samples. When a water droplet was dropped onto the etched steel surface, it spread onto the sample surface very quickly, indicating the superior superhydrophilic property of the sample surface (Fig. 3b). This is in line with the very low contact angle, 10°, of the as-prepared etched sample surface composed of FeF_3. Whereas nonetched steel substrate has a contact angle of ca. 93° (Fig. 3a), the high hydrophilicity of etched one may be related to micro- and nanostructure formed on surface by deposition of fluoride and oxide. It could be also due to the removal of surface adventitious hydrocarbon contamination. In metalworking process, HF is commonly used as a pickling agent to remove oxides and adventitious hydrocarbon contamination from stainless and carbon steels.

The etched steel surface became superhydrophobic after simply immersing the sample in an ethanol solution containing stearic acid for 24hr. Fig. 3d shows the water droplet behavior on the etched steel surfaces after stearic acid coating. The static water contact angle of these modified sample surfaces was found to be 155°, clearly revealing that the surface changed from superhydrophilic to superhydrophobic. Besides, a water droplet can hardly be attached to the super-hydrophobic surface, as indicated by a sliding angle of around 10°. Whereas CA is only 109° for nonetched steel after stearic acid coating, it indicates that nano- and micro-scale structures through the deposition of FeF_3 on the steel surface play great role in determining wetting properties of superhydrophobic surfaces.

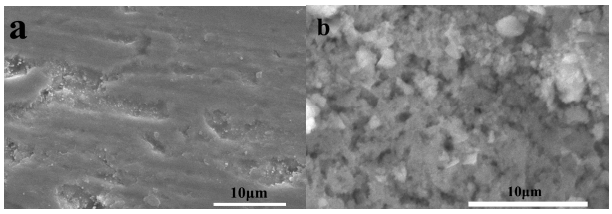

Fig. 2 SEM images of steel (a) before and (b) after chemical etch

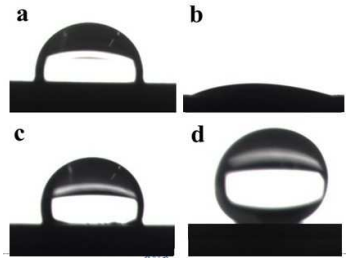

Fig. 3 Water droplet image on (a) nonetched steel, (b) etched steel, (c) stearic acid film on nonetched steel, and (d) stearic acid film on etched steel

It is known that the surface wettability is controlled by the chemical composition and surface roughness of solids. [35] The water contact angle of a smooth surface can reach ca. 120°, but on the micropatterned surface or hierarchical structures, the water contact angles can reach a maximum value of ca. 178°. [36] This suggests that the fabrication of the hierarchical structures is a crucial factor in the fabrication of superhydrophobic surfaces. Our fabricated surface, based on chemical etch and stearic acid coating, showed an advancing water contact angle of more than 150° and a sliding angle of 10°. These results support the fact that the water droplets do not penetrate into the grooves. Thus, micro and nano-scale structures based on deposition of FeF_3 nanosheets not only enhance the surface hydrophobicity but also reduce the contact angle hysteresis by decreasing the contact area between the solid and liquid at their interface and the continuity of the three-phase contact line at the solid-liquid interface. Fractional surface coverage for the solid surface in contact with water, f_s, can be estimated by using Cassie and Baxter equation [37]

$$\cos\theta_w = f_s \cos\theta_s - (1 - f_s) \quad (1)$$

Where θ_w and θ_s represent the water CAs on rough and smooth surfaces, respectively. Here θ_w =93° and θ_s=155°, so fs is determined to be about 0.10 according to equation (1). It corresponds to a fraction of 0.90 of air trapped within the interstices of the nanotextured surface. Such a large fraction of

trapped air results in a significantly increased area of the air/water interface, thereby effectively preventing water droplets from penetrating into the grooves on the hydrophobic surface.

Frictional behavior of superhydrophobic steel

To apply superhydrophobic surfaces to industrial fields, it is very important to reveal the mechanical stability of the superhydrophobic film. So far, there is no a single, standardized test method to characterize the abrasion resistance of superhydrophobic surfaces. Most studies utilize custom-built in-house setups that involve rubbing the superhydrophobic specimen against materials such as cloth, [38] sandpaper [39] or synthetic leather [40] under a certain load. Likewise, no single measure has been used for characterizing the durability of superhydrophobic surface. Different criteria used in the literature include the change in contact angle hysteresis, [38] water shedding angle, [39] roll-off behavior, [41]. Because we are interested in frictional behavior of superhydrophobic film on steel, a ball-on-flat tribometer experiments were conducted to characterize the durability of superhydrophobic surfaces. This is important because, for some tribological application, the friction also needs to be as low as possible in order to minimize frictional energy consumption and reduce wear. In the test, a steel ball is sliding against superhydrophobic surface under a certain load. In this case, change of friction coefficient could be used to characterize the durability for superhydrophobicity. Generally, lower friction could be always observed if the protective superhydrophobic film existed on the surface. However, when the layers had worn off, ruptured, or broken down, the friction coefficient sharply increased to a lager value. Therefore, the sliding time that could be applied to the protective superhydrophobic film before the friction rose was used to characterize life of the superhydrophobic film.

Fig. 4 shows the evolution of friction coefficient versus the sliding time for steel under different treatments in sliding against an AISI52100 steel ball at load of 1N and sliding speed 0.5m/s. First, the friction behavior of nonetched steel was investigated. High friction was immediately observed after sliding. The nonetched steel displays initial coefficient of friction of 0.20 and sharply increase to 0.60 after ~20s sliding (curve a of Fig. 4). It was assumed that surface failure occurred when protective layers (i.e. surface oxide) on steel had worn off, ruptured, or broken down.

It was also important to know if the chemical etch process itself changed the frictional behavior of steel. As shown in curve b in Fig. 4, the etched steel shows some better friction reducing performance, as comparing to nonetched steel. The initial friction coefficient is as low as 0.12 and can be remained for about 200 s sliding before sharply increasing to 0.5.

The effect of stearic acid coating on the friction-reducing performance of nonetched steel is also investigated. As compared to the nonetched steel (curve a in Fig. 4), the stearic acid film on the nonetched steel shows better tribological performance (curve c in Fig. 4). The initial friction coefficient reduces to 0.1. However, the low friction coefficient can only remains in a short period and then it sharply increases to 0.30, corresponding to failure of stearic acid film on the nonetched steel substrate.

Now it is time to test the friction-reducing performance of superhydrophobic steel surface which integrates the chemical etch and stearic acid coating. Surprisingly, after the stearic acid film is formed atop the etched steel, the as-obtained superhydrophobic steel surface shows the great improvement in tribological performance. At load of 1N, the initial friction coefficient can be as low as 0.12 and the low friction coefficient can remains for 7200s before the experiment stops due to long test duration (curve d in Fig 4). It strongly indicates that excellent friction reducing performance with drastically increased durability can be achieved by combining the beneficial effects of chemical etch and stearic acid film.

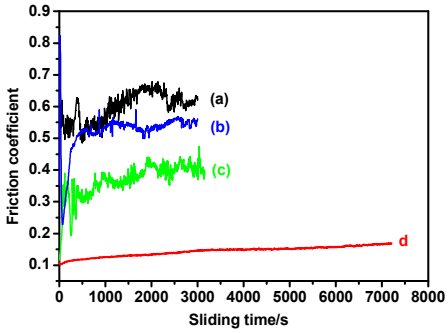

Fig. 4 Friction coefficient vs sliding time curves for various samples at load of 1N. (a) nonetched steel, (b) etched steel, (c) stearic acid film on nonetched steel, and (d) stearic acid film on etched steel

The effect of applied loads on the friction reducing performance of superhydrophobic steel is also investigated. As shown in Fig. 5, even the load is increased to 4N with Hertz contact pressure of 1.36 GPa, the superhydrophobic steel surface can maintain lower friction for 1500s.

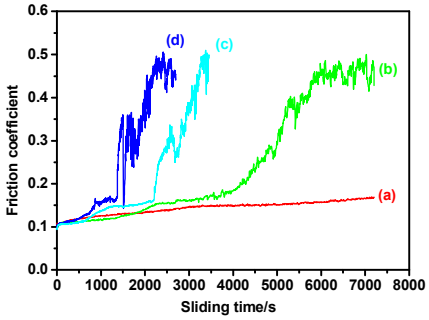

Fig. 5 Friction coefficient vs sliding time curves for stearic acid film on etched steel at load of (a) 1N, (b) 2N, (c) 3N and (d) 4N

Discussion

Up to now, research on superhydrophobic materials has mostly focused on their extreme non-wettability and its related self-cleaning [13,14], anticorrosion [15-17], anti-icing [18-24] performances. The surface wettability is controlled by both the chemical composition and surface roughness of solids. Generally, a superhydrophobic behaviour can be determined only if surface simultaneously possesses low surface energy and elevated roughness. However, the superhydrophobic surfaces with a large roughness commonly show poorer mechanical properties than flat surfaces. The loss of roughness increases the area of contact between water and the surface. Furthermore, the intrinsic hydrophobicity of the surface is reduced as a result of hydrophilic contamination or damage to a hydrophobic surface layer. As a consequence, the superhydrophobic state may become unstable or

contact angle hysteresis may increase. It was found that the non-wettability of a superhydrophobic surface can be reduced essentially when such a surface is used underwater [42]. Other studies found that the ice adhesion of superhydrophobic surfaces slightly increased after they was undergone several icing/ice-breaking cycles, due to a minor damage of the surface nano/microstructure and the coating layer upon these multiple ice-breaking and ice-melting processes [18-24].

In this manuscript, we present a simple two-step route to construct superhydrophobic surfaces on steel. Namely, a rough surface with a certain micro- and nanometer-scale structures is prepared at the first step to trap a large amount of air and to reduce the contact area between water and a solid surface. Though a number of methods have been proposed to construct surface roughness on steel, including electrochemical deposition [43-46], sol–gel coating [47-49], layer-by-layer assembly [50-52] and chemical vapour deposition [53, 54], they mostly establish roughness by the deposition of particles or residues on surface. Chemical etch is used here to create surface roughness. The key advantage of such a technique is to generate roughness directly on steel, which is the inherent mechanical stability of the structures that are formed. Here, HF/H_2O_2 solution is used to create the nano- and microscale texture on surface of carbon steel. According to SEM images in Fig. 2, the etched steel shows twofold increase in surface roughness. The rough surface can trap a large fraction of air within the micro- and nanotextured surfaces. The trapped air can greatly increase the air-liquid interface, which prevents the water droplets from penetrating into the grooves of the surfaces.

The as-obtained rough surface visa chemical etch is then coated with a stearic acid film in the second step to achieve superhydrophobic properties to steel surface. Recently, self-assembled films of n-alkanoic acids have been used to render metal surface super-hydrophobicity [55-57]. Another reason for using stearic acid as low surface energy film is that fatty acids, dispersed in lubricating base oil, have been used as model friction modifiers for a long time [58]. The first and so far the most authoritative explanation of friction-reducing phenomenon from fatty acids emerged from the work of Bowden and Tabor [59]. The fatty acid molecules are chemically adsorbed on the metal substrate surface and then transformed under tribological condition to a layer of fatty soaps by chemical reaction with the substrates. Low friction was obtained when such a layer was sliding against a solid counterface under certain conditions [60–62]. This might attributed to the fact that stearic acid formed molecular assemblies in which one end of the long-chain molecules is attached to the substrate surface by COOH group. The alkyl chains may thus have a significant freedom of swing and rearrange along the sliding direction under shear stress, and therefore yield a smaller resistance. In addition, the lower surface energy of stearic acid film on steel, as indicated by larger CA, might be another important reason for the lower friction.

Therefore, this research integrates chemical etching and stearic acid coating to produce superhydrophobic surfaces on steel for the purpose of reducing friction forces in sliding contact. In this regard, stearic acid film is deposited on the etched steel substrate. Surprisingly, the great improvement in tribological performance is observed. It is clear that the etched steel is high hydrophilicity, possessing a hydroxyl-enriched, or a hydroxylated surface which is more easily reacted with stearic acid. Furthermore, rougher surface of etched steel could provide more reactive space for adsorption and reaction of stearic acid molecules. As a result, it is reasonable to suggest a densely packed stearic acid film is formed on the etched steel surface, leading to significantly improved low friction with extended durability.

Briefly, it is feasible to drastically enhance the tribological durability of steel by combining friction-reducing effects of surface texture from rough surface and low energy surface from stearic acid film. This finding, hopefully, will open a new route to superhydrophobic surfaces with low friction and good durability, providing meaningful guidance to the application of various engineered surfaces and interfaces.

Experimental

Preparation of superhydrophobic film on steel

AISI 1045 steel samples were commercially obtained in the form of 10×20×2mm coupons and mechanically polished to a mirror finish with Ra=24nm. Etching was performed at 25 °C using a 1:1 mixture of hydrofluoric acid (48%)-hydrogen peroxide(30%) for 10 seconds. *Great care should be exercised when preparing and handling this highly aggressive solution. The mixing is an exothermic process, and a violent decomposition reaction can occur when mixing large amounts of these chemicals.*

The textured steel samples were briefly rinsed with water and ethanol, immersed in an ethanolic solution containing 0.01 mol/L stearic acid at ca. 25 ^{o}C for 24 h. Upon completion, the steel substrates were lifted from the solution and then sonicated several times in ethanol to remove all physisorbed materials, yielding superhydrophobic surfaces after fully drying in air.

Contact angle measurements.

CA measurements were conducted under static condition with a remote computer-controlled goniometer system (CAM101, KSV Instruments Ltd.). The drop volume was about 5μL in this study. Deionized water droplets were prepared at different locations of the to-be-tested surfaces by using a syringe. All CA measurements were run under ambient laboratory conditions (temperature about 25 °C, relative humidity about 40 %); and five repeat measurements were carried out for each sample. Images of water droplets were analyzed using Imagetool software (University of Texas Health Science Center) to measure CA. Sliding angle measurements were made using a simple instrument fabricated in our laboratory. It consisted of a smooth and planar platform on which the sample was placed. The angle at which the drop slides can be measured by means of a protractor attached to the instrument.

Profilometer measurements

The morphological properties of the samples' surfaces were performed with Atomic Force Microscope (AFM, Shimadzu SPM-9500). Typically, a tapping mode was utilized that is known to provide optimal performance in such cases.

Surface analysis

The surface chemical structure of steel surface is confirmed by

an X-ray photoelectron spectroscopy (Kratos AXIS ULTRA, UK) employing a microfocused Al Kα monochromatic X-ray source (1486.6 eV) with a 400μm spot size. Scanning electro microscopy (SEM) images were taken with a Hitachi S-3500N SEM.

Ball-on-plate experiments

Unlubricated friction and wear tests were carried out using a ball-on-plate tribometer, including a ball upper specimen that slides against a flat lower specimen. The counterpart was commercially available AISI52100 bearing steel ball with the diameter of 4 mm. The hardness of AISI52100 steel ball was HRc 62-63 and surface roughness Ra is 0.1μm. For each test a new ball was employed. The flat was mounted on a reciprocating driver and moved back and forth during the test. The upper ball was relatively stable during test. Normal load was applied downward through the upper ball specimen against the flat. In order to keep constant normal load, a vertical fine adjusting movement of the ball was allowed during the test. The friction coefficient was calculated from friction force and normal force, which were measured by the load sensor and recorded by a PC automatically.

Test conditions including normal load, average velocity, reciprocating stroke length, frequency, total distance, humidity and temperature are listed in Table 1. Each testing condition was repeated three times. The average friction coefficient is cited in this article.

Conclusions

Micro/nano-engineered surfaces by chemical etch and stearic acid modification were fabricated on steel. The effects of stearic acid modification and surface micro/nano-texturing by chemical on the wetting and frictional properties of steel substrates were studied. The results show that the combination of stearic acid modification and micro/nano-texturing can create superhydrophobic surfaces with a water CA of 155° and a sliding angle of smaller than 10°. This study also shows that excellent friction reducing performance with drastically increased durability can be achieved for such a superhydrophobic surface.

Table 1 The friction and wear test conditions

Normal load (N)	1.0	2.0	3.0	4.0
Hertz contact pressure (GPa)	0.86	1.08	1.23	1.36
Average velocity (m/s)	0.024			
Frequency (Hz)	2			
Stroke length (mm)	6			
Humidity (%)	40–50			
Temperature (◦C)	ca. 25			

Acknowledge

Financial support by National Natural Science Foundation of China (51375249) is gratefully acknowledged.

Notes and references

[a] *School of Mechanical Engineering, Qingdao Technological University, Qingdao 266033, P. R. China. Tel &Fax: +86 532 85071980; E-mail: wanyong@qtech.edu.cn*

[b] *State Key Laboratory of Solid Lubrication, Lanzhou Institute of Chemical Physics, Chinese Academy of Sciences, Lanzhou 730000, P. R. China*

1 W. Barthlott and C. Neinhuis, *Planta,* 1997, **202**, 1
2 E. Celia, T. Darmanin, E. T. de Givenchy, S. Amigoni and F. Guittard, *J. Colloid Interface Sci.*, 2013, **403**, 1
3 X. J. Feng, and L. Jiang, *Adv. Mater.*, 2006, **18**, 3063
4 X.-M. Li, D. Reinhoudt and M. Crego-Calama, *Chem. Soc. Rev.,* 2007, **36**, 1350
5 P. Roach, N. J. Shirtcliffe and M. I. Newton, *Soft Matter*, 2008, **4**, 224
6 Z. Guo, W. Liu and B.-L.Su, *J. Colloid Interface Sci.*, 2011, **353**, 335
7 A. Lafuma and D. Quéré, *Nat. Mater.*, 2003, **2**, 457
8 M. Miwa, A. Nakajima, A. Fujishima, K. Hashimoto and T. Watanabe, *Langmuir*, 2000, **16**, 5754
9 M. Nosonovsky and B. Bhushan, *Curr. Opin. Colloid. Interface Sci.*, 2009, **1**4, 270
10 A. Otten and S. Herminghaus, *Langmuir,* 2004, **20**, 2405
11 Y.-L. Zhang, H. Xia, E. Kim, and H.-B. Sun, *Soft Matter*, 2012, **8**, 11217.
12 M. Qu, B. Zhang, S. Song, L. Chen, J. Zhang and X. Cao, *Adv. Funct. Mater.*, 2007, **17**, 593
13 R. Blossey, *Nat. Mater.*, 2003, **2**, 301
14 R. Fürstner, W. Barthlott, C. Neinhuius and P. Walzel, *Langmuir,* 2005, **21**, 956
15 T. Ishizaki, N. Saito, Y. Inoue, M. Bekke and O. Takai, *J. Phys. D: Appl. Phys.*, 2007, **40**, 192
16 H. Q. Liu, S. Szunerits, W. G. Xu, and R. Boukherroub, *ACS Appl. Mater. Interfaces*, 2009，1, 1150.
17 F. Zhang, L. Zhao, H. Chen, S. Xu, D. G. Evans, and X. Duan, *Angew. Chem. Int. Ed. Engl.*, 2008, 47, 2466
18 L. B. Boinovich, A. M. Emelyanenko, V. K. Ivanov, and A. S. Pashinin, *ACS Appl. Mater. Interfaces*, 2013, **5**, 2549.
19 M. Ruan, W. Li, B. Wang, B. Deng, F. Ma, and Z. Yu, *Langmuir*, 2013, **29**, 8482.
20 S. B. Subramanyam, K. Rykaczewski, and K. K. Varanasi, *Langmuir*, 2013, **29**, 13414.
21 L. Cao, A. K. Jones, V. K. Sikka, J. Wu, and D. Gao, *Langmuir*, 2009, **25**, 12444.
22 S. Farhadi, M. Farzaneh, and S. A. Kulinich, *Appl. Surf. Sci.*, 2011, **257**, 6264
23 S. A. Kulinich and M. Farzaneh, *Langmuir*, 2009, **25**, 8854.
24 S. A. Kulinich and M. Farzaneh, *Cold Reg. Sci. Technol.*, 2011, **65**, 60
25 P. L. Menezes, Kshore, S.V Kailas and M. R. Lovell, *Tribol. Lett.*, 2011, **41**, 1
26 M. Shafiei and A. T. Alpas, *Appl. Surf. Sci.*, 2009, **256**, 710
27 M. Zou, L. Cai and H. Wang, *Tribol. Lett.*, 2006, **21**, 25
28 B. Bhushan and Y. C. Jung, *Nanotechnology*, 2006, **17**, 2758
29 S. P. Pujari, E. Spruijt, S. M. A, Cohen C. J. van Rijn, J. M. Paulusse and H. Zuilhof., *Langmuir*. 2012, **28**, 17690
30 Y. Song, R. P. Nair, M. Zou and Y.A.Wang, *Thin Solid Films*, 2010, **518**, 3801
31 E.-S.Yoon, R. A. Singh, H.-J. OH and H. Kong, *Wear*, 2005, **259**, 1424
32 C. Pham, K. Na, S. Piao, I.-J. Cho, K.-Y. Jhang and E.-S. Yoon, *Nanotechnology*, 2011, **22**, 395303
33 Y. Wan, Z. Wang, Y. Liu, C. Qi and J. Zhang, *Tribol. Lett.*, 2011, **44**, 327
34 L. Li, V. Breedveld, and D. W. Hess, *ACS Appl. Mater. Interfaces*, 2012, **4**, 4549.
35 M. Callies, D. Quere, *Soft Matter,* 2005, **1**, 55.
36 E. Hosono, S. Fujihara, I. Honma, H. Zhou, *J. Am. Chem. Soc.* 2005, **127**, 13458.
37 A. Cassie, S. Baxter, *Trans. Faraday Soc.* 1944, **40**, 546.
38 Y. Xiu, Y. Liu, D. W. Hess, and C. P. Wong, *Nanotechnology*, 2010, **21**, 155705
39 I. S. Bayer, A. Brown, A. Steele, and E. Loth, *Appl. Phys. Express,* 2009 , **2** , 5003
40 J. Zimmermann, F. A. Reifler, G. Fortunato, L. Gerhardt, and S. Seeger, *Adv. Funct. Mater.* 2008 , **18** , 3662.
41 B. Basu, and A. Paranthaman, *Appl. Surf. Sci*. 2009, **255**, 4479

42 X. Sheng, J. Zhang, *Colloids Surf. A Physicochem. Eng. Asp.*, 2011, **377**,. 374–378
43 F. Shi, Z. Wang and X. Zhang, *Adv. Mater.* 2005, **17**, 1005.
44 T. Darmanin, E. Taffin de Givenchy, S. Amigoni and F. Guittard, *Adv. Mater.*, 2013, **25,** 1378.
45 H. Yan, K. Kurogi, H. Mayama and K. Tsujii, *Angew. Chem., Int. Ed.*, 2005, **44**, 3453.
46 M. Wolfs, T. Darmanin and F. Guittard, *RSC Adv.*, 2013, **3,** 647;
47 Tadanaga, J. Morinaga, A. Matsuda and T. Minami, *Chem. Mater.* 12 (2000) 590.
48 M. Manca, A. Cannavale, L. De Marco, S. A. Arico, R. Cingolani and G. Gigli, *Langmuir*, 2009, **25,** 6357.
49 Q. F. Xu, J. N. Wang and K. D. Sanderson, *ACS Nano*, 2010, **4**, 2201.
50 F. Zhai, F. C. Cebeci, R. E. Cohen and M. F. Rubner, *Nano Lett.*, 2004, **4,** 1349.
51 R. M. Jisr, H. H. Rmaile and J. B. Schenoff, *Angew. Chem., Int. Ed.*, 2005, **44**, 782.
52 S. Amigoni, E. T. de Givenchy, M. Dufay and F. Guittard, *Langmuir*, 2009, **25**, 11073.
53 J. P. Lee, S. Choi and S. Park, *Langmuir*, 2011, **27**, 809.
54 A. Pakdel, C. Zhi, Y. Bando, T. Nakayama and D. Golberg, *ACS Nano*, 2011, **5**, 6507.
55 L. Feng, H. Zhang, P. Mao, Y. Wang and Y. Ge, *Appl. Surf. Sci.*, 2011, **257**, 3959
56 Y. C. Hong, S. C. Cho, D. H. Shin, S. H. Lee and H. S. Uhm, *Scripta Mater.*, 2008, **59**, 776
57 S. Wang, L. Feng and L. Jiang, *Adv. Mater.*, 2006, **18**, 767
58 D. Dowson, History of tribology, Professional Engineering Publishing, London, 1998.
59 F. P. Bowden and D. Tabor, Friction and lubrication, 2nd edn., Methuen & Co Press, London, 1967.
60 R. R. Sahoo and S. K. Biswas, *J. Colloid Interface Sci.*, 2009, **333**, 707.
61 S. M. Lundgren, M. Ruths, K. Danerlöv and K. Persson, *J. Colloid Interface Sci.*, 2008, **326**, 530.
62 M. Ruths, S. Lundgren, K. Danerlöv and K. Persson, *Langmuir*, 2007, **24**, 1509.